Electronic Supplementary Material (ESI) for Journal of Materials Chemistry A.

Supporting Information

A high energy density Li-rich positive-electrode material with superior performances *via* a dual chelating agent co-precipitation route

PeiyuHou, Long Xu,Jishun Song, Dawei Song,[*]*Xixi Shi, Xiaoqing Wang and Lianqi Zhang*[*]

Experimental section

The preparation of precursors and Li-rich layered materials. To synthesize the new hydroxide precursors, stoichiometric $NiSO_4 \cdot 6H_2O$, $CoSO_4 \cdot 7H_2O$, and $MnSO_4 \cdot H_2O$ (cationic ratio of Ni:Co:Mn=3:1:6) were dissolved with a concentration of 2.0 mol L^{-1} as the starting materials. Then the aqueous solution was pumped into a continuously stirred tank reactor (CSTR, capacity of 10 L) under a nitrogen atmosphere and reacted with 5 mol L^{-1}NaOH solution (aq) as the pH control agent, 0.5 mol L^{-1} NH_4OH and 0.02 mol L^{-1} $H_2C_2O_4$ solution (aq) as dual chelating agents in the reactor under 50 °C and constant pH (11.0) with 600rpm stirring rate, leading to the new precursors $[Ni_{0.3}Co_{0.1}Mn_{0.6}](OH)_2$. And the normal precursors $[Ni_{0.3}Co_{0.1}Mn_{0.6}](OH)_2$ was also achieved via a similar co-precipitation route without $H_2C_2O_4$ chelating agent. Then, both as-prepared $[Ni_{0.3}Co_{0.1}Mn_{0.6}](OH)_2$ particles were filtered, washed, and dried 24 h in air. The obtained new and normal precursor particles were calcined with stoichiometric ratio Li_2CO_3 (Li/M=1.3) at high temperaturein a furnace under air to form layered new and normal Li-rich materials.

Materials characterization. Precursors products were collected at the end of the co-precipitation experiment and the particle size distribution was measured with a particle size analyzer (OMEC, LS-POP(6)). X-ray Diffractometry (XRD, Rigaku D/MAX-2500) was employed to characterize structure of the prepared materials. XRD data were obtained at 2θ=10-80° with a step size of 0.02°, using Cu Kα radiation. The morphology of synthesized materials was observed by a Scanning Electron Microscope (SEM, Hitachi S4800). Energy Dispersive X-ray Spectroscopy (EDS, Hiroba EDX) and X-ray photoelectron spectroscopy (XPS, PHI5000 VersaProbe) was used to analyse surface chemical composition and valence of lithiated materials. High resolution transmission electron microscopy (HRTEM) characterization data were conducted using a 200 kV JEOL-JEM 2100 transmission electron microscope.

For Differential Scanning Calorimetry (DSC) experiments, cells were finally charged to 4.8 V at a constant current density of 20 mA g^{-1} at 25 °C and opened carefully in the Ar-filled dry box. After opening the cells, the electrode materials were recovered from the current collector. The DSC datas were collected in a Differential Scanning Calorimeter (NETZSCH 204F1) using a scan rate of 5 °C min^{-1} in the range of 50-350 °C.

Electrochemical measurements. For fabrication of positive electrodes, the prepared materials were mixed with acetylene black and PVDF (80:10:10 in weight) in NMP. The obtained slurry was coated onto Al foil and dried at 80 °C for a day, followed by a roll-pressing. After drying, positive disks of 0.785 cm^2 area were punched out to assemble the coin cells. The electrodes consisted of a similar active material loading of 4.5-5.0 mg cm^{-2}. Prior to use, the electrodes were dried again at 120 °C for half a day in a vacuum oven. The electrodes were electrochemically characterized using a 2032 type of coin cell with lithium foil as the anode and 1 M $LiPF_6$ in ethylene carbonate diethyl carbonate (3:7 in volume) as the electrolyte. The cells were preliminarily charged and discharged in the range of 2.0-4.8 V (versus Li/Li^+) at 25 °C.

Electrochemical impedance spectra (EIS) were measured using a Zahner IM6ex electrochemical workstation in the frequency range of 100 kHz to 10 mHz.

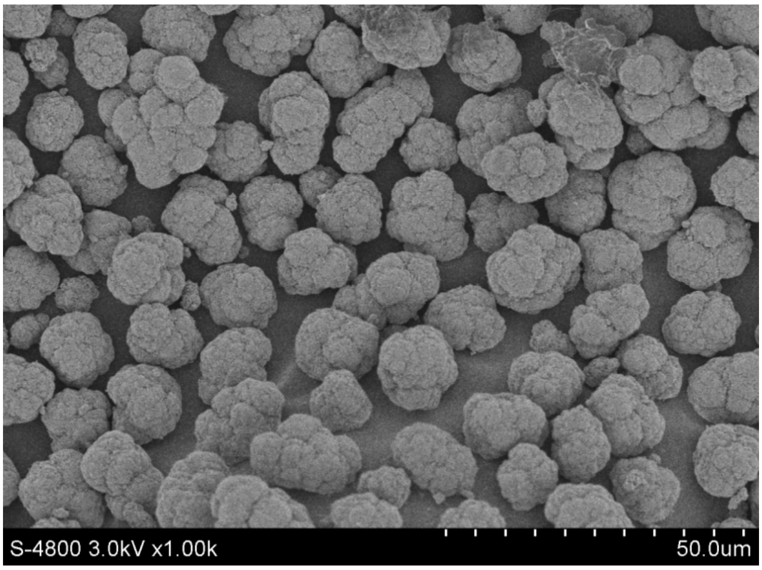

Fig. S1 SEM image of the new hydroxide precursors prepared *via* a dual ammonia and oxalate chelating agent route.

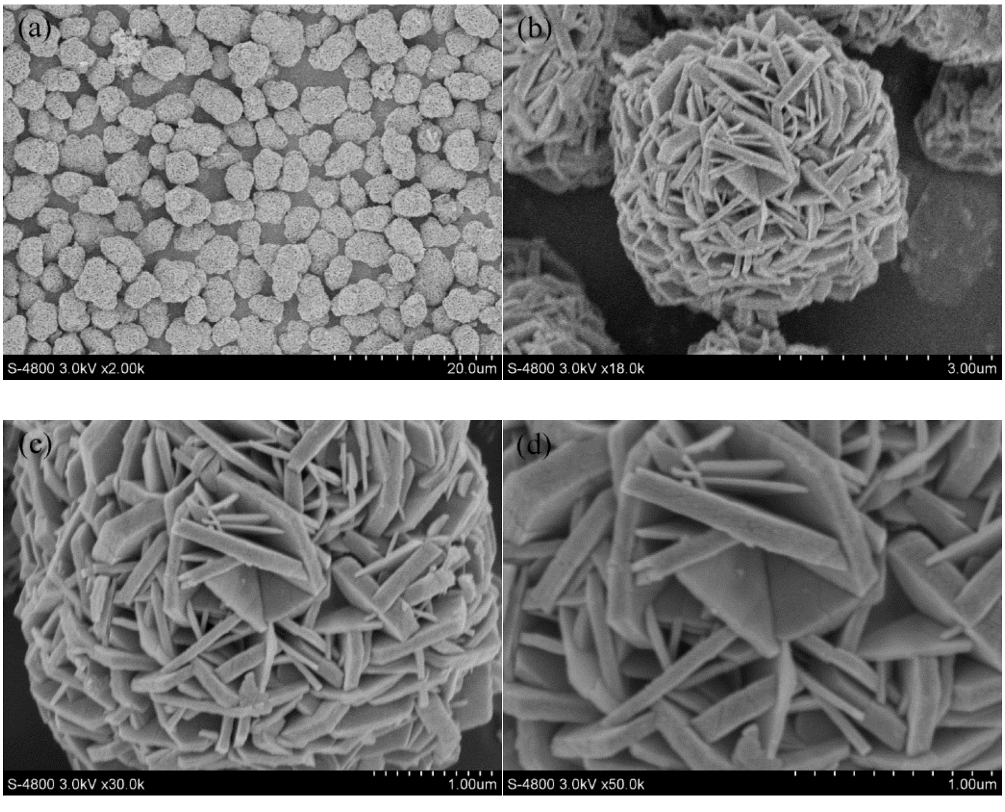

Fig. S2 SEM images of the normal hydroxide precursors prepared *via* an ammonia chelating agent route.

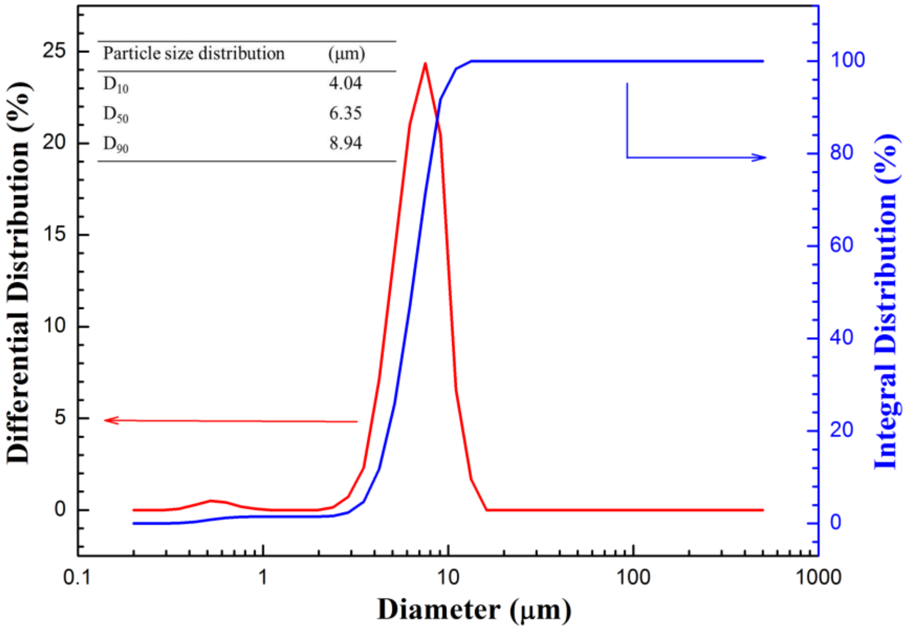

Fig. S3 Particle size distribution of the normal hydroxide precursors prepared *via* an ammonia chelating agent route.

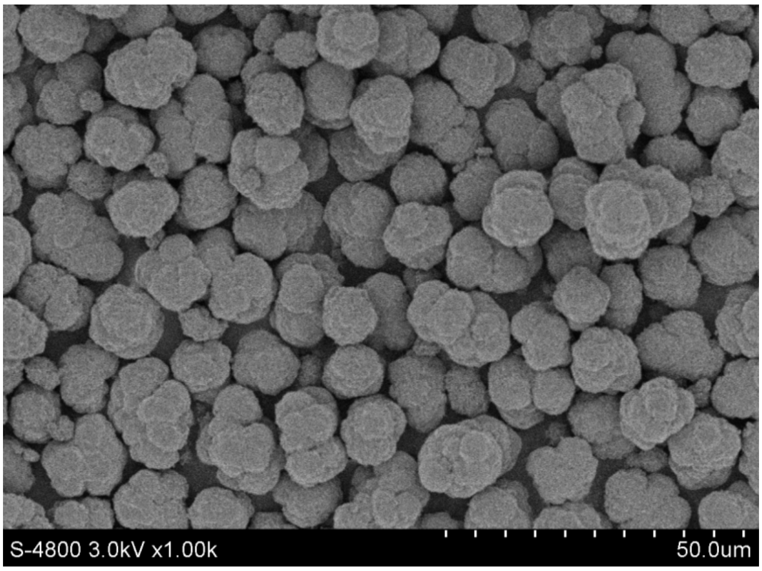

Fig. S4 SEM image of the new Li-rich layered materials from hydroxide precursors prepared *via* a dual ammonia and oxalate chelating agent route.

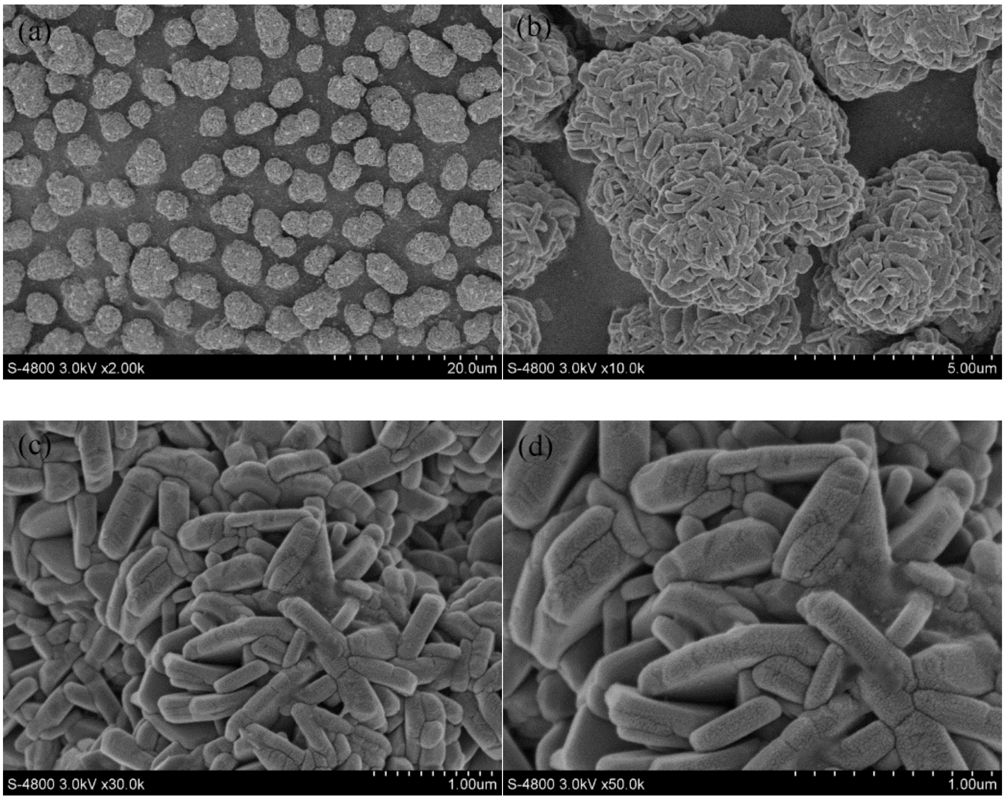

Fig. S5 SEM images of the normal Li-rich layered materials from the hydroxide precursors prepared *via* an ammonia chelating agent route.

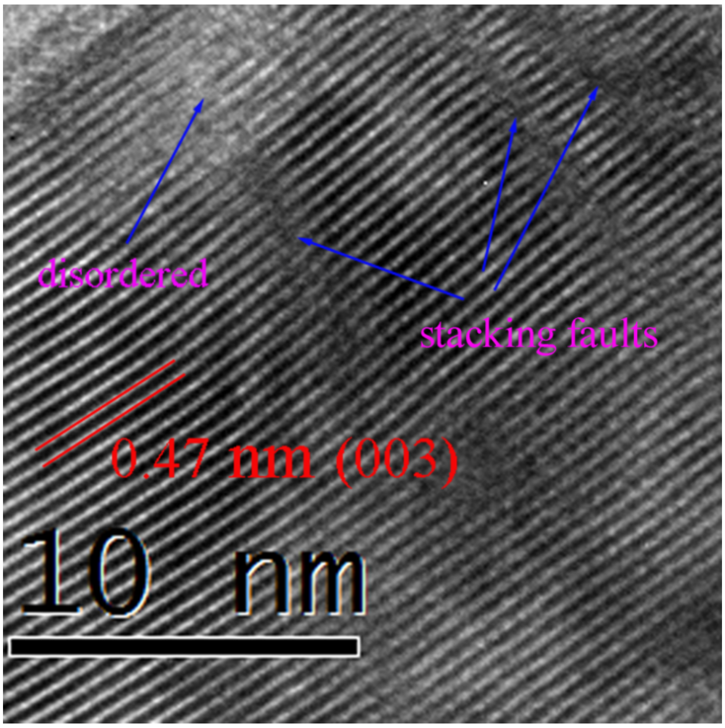

Fig. S6 TEM image the normal Li-rich layered materials from the hydroxide precursors prepared *via* an ammonia chelating agent route.

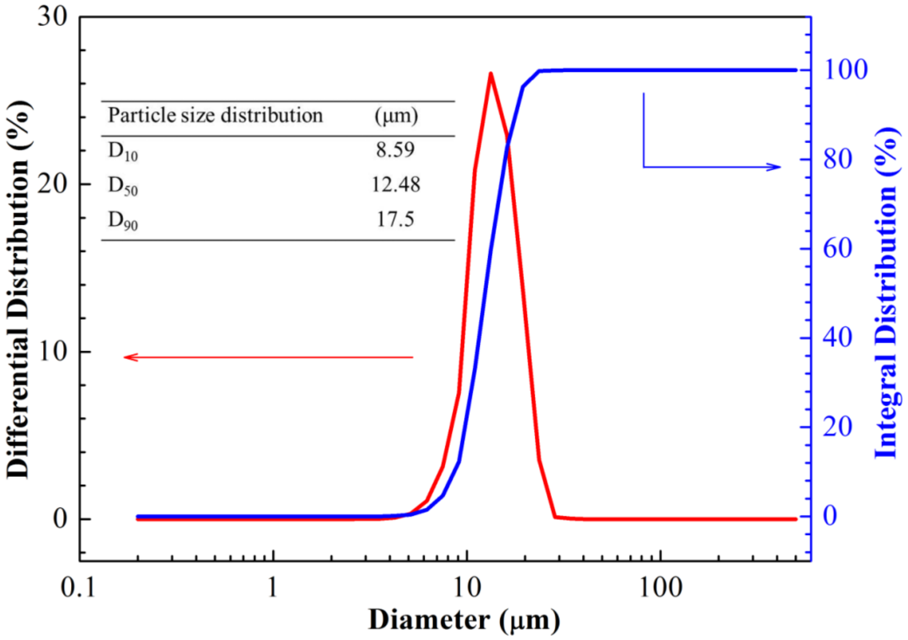

Particle size distribution	(μm)
D_{10}	8.59
D_{50}	12.48
D_{90}	17.5

Fig. S7 Particle size distribution of the new Li-rich layered materials from the hydroxide precursors prepared *via* a dual ammonia and oxalate chelating agent route.

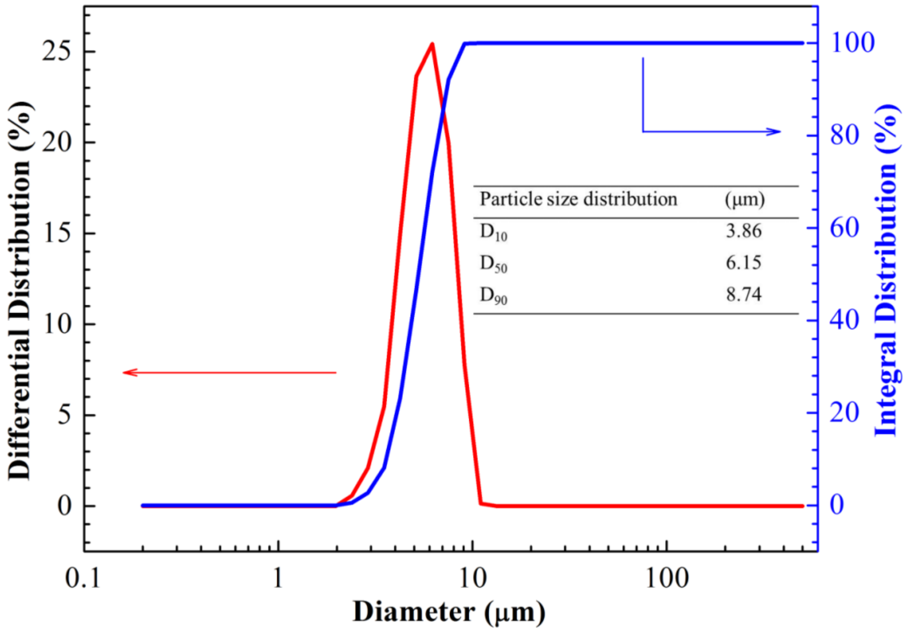

Particle size distribution	(μm)
D_{10}	3.86
D_{50}	6.15
D_{90}	8.74

Fig. S8 Particle size distribution of the normal Li-rich layered materials from the hydroxide precursors prepared *via* an ammonia chelating agent route.

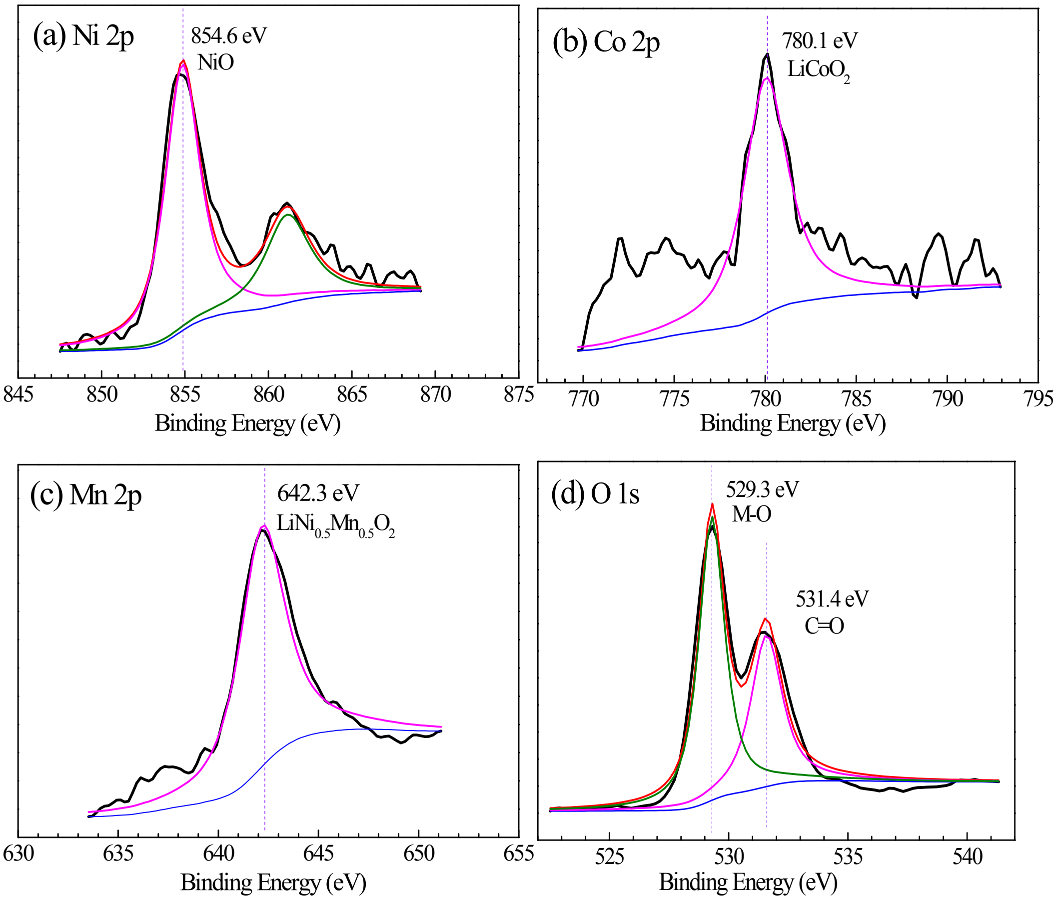

Fig. S9 XPS spectra of the new Li-rich layered materials from the hydroxide precursors prepared *via* a dual chelating agent route: (a) Ni 2p spectrum, (b) Co 2p spectrum, (c) Mn 2p spectrum and (d) O 1s spectrum.

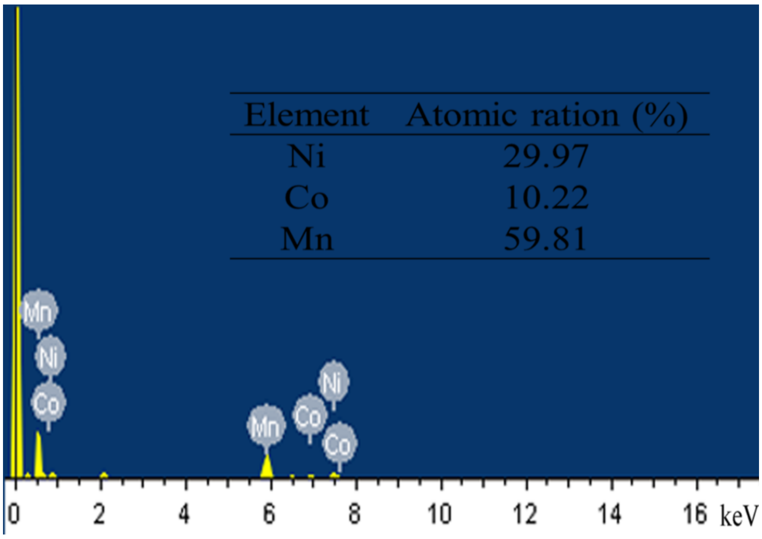

Element	Atomic ration (%)
Ni	29.97
Co	10.22
Mn	59.81

Fig. S10 EDS of the as-prepared new Li-rich materials from the new hydroxide precursors prepared via a dual chelating agent route.

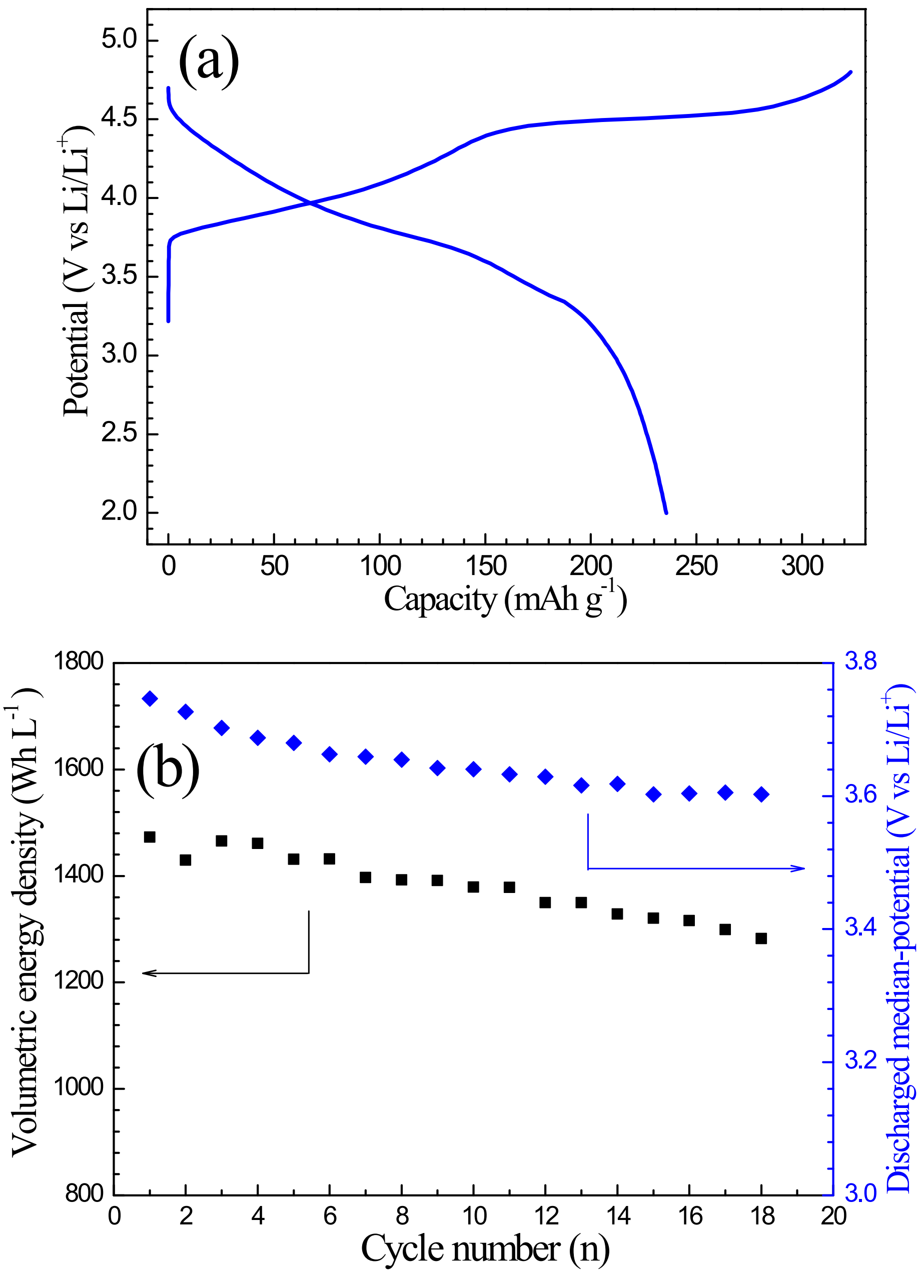

Fig. S11 The (a) initial charge-discharge curve and (b) cycle life of the normal Li-rich layered materialsfrom the hydroxide precursors prepared *via* an ammonia chelating agent route in the range of 2.0-4.8 V at a current density of 10 mA g^{-1} (0.046 mA cm^{-2}).

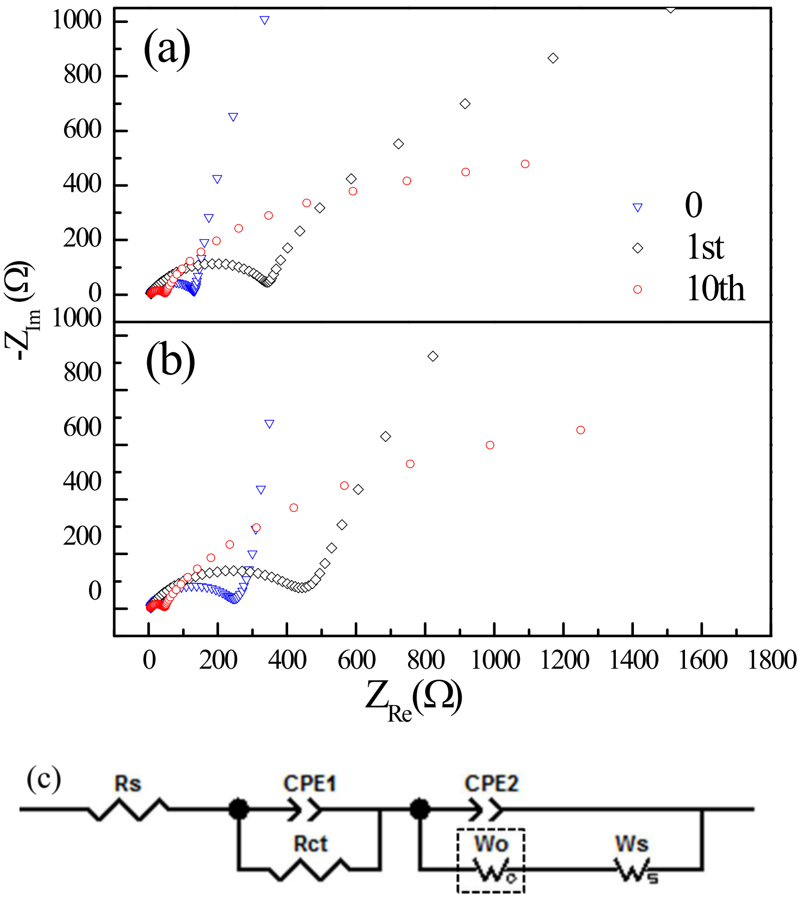

Fig. S12 Impedance spectra of the (a) normal Li-rich oxides from the hydroxide precursors prepared via an ammonia chelating agent, (b) new Li-rich oxides from the hydroxide precursors prepared *via* a dual chelating agent routeand (c) equivalent circuits used to fit the experimental data. Rs is solution resistance, Rct is charge-transfer resistance, CPE1 and CPE2 are constant phase element, Ws and Wo are assigned to the finite Nernst diffusion impedance in the thin film and semi-infinite Warburg diffusion impedance in the bulk, respectively.

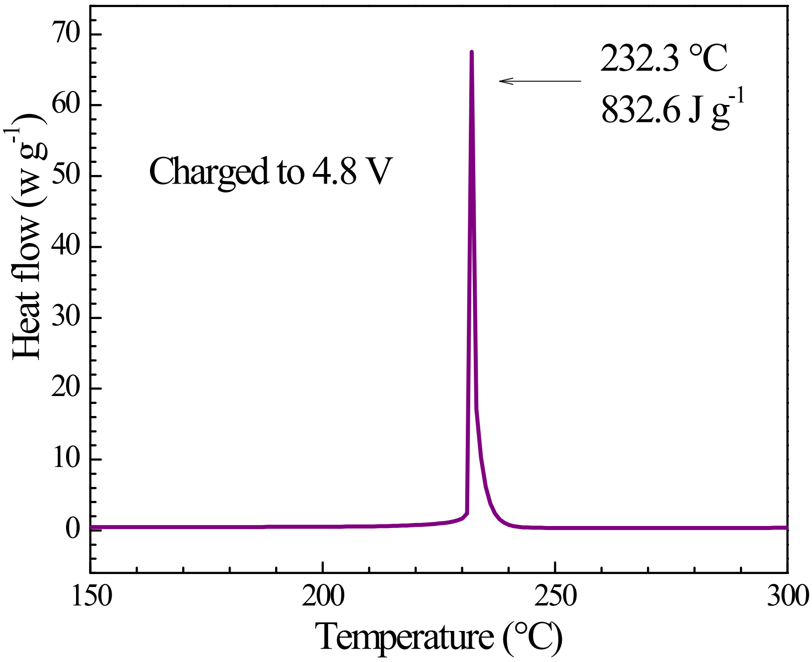

Fig. S13 DSC curve of the normal Li-rich materials from the hydroxide precursors prepared via an ammonia chelating agent.

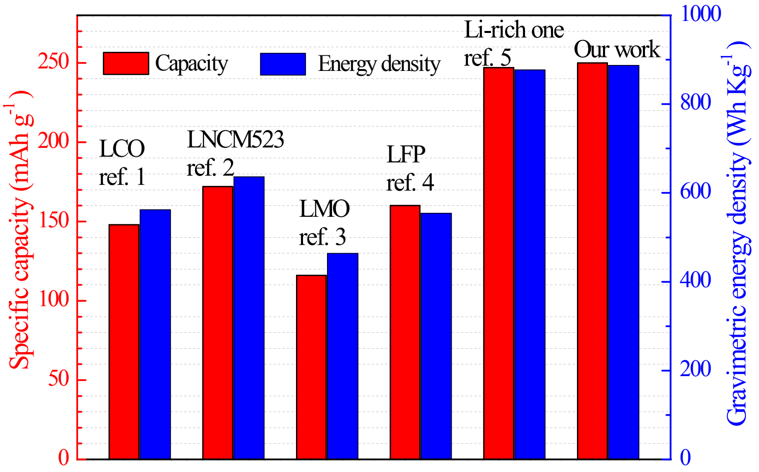

Fig. S14 Gravimetric energy density and specific capacity comparison of these common layered, spinel and olivine positive-electrode materials including $LiCoO_2$ (LCO), $LiNi_{0.5}Co_{0.2}Mn_{0.3}O_2$ (LNCM523), $LiMn_2O_4$ (LMO), $LiFePO_4$ (LFP), previous reported Li-rich material $Li_{1.19}(Ni_{0.16}Co_{0.08}Mn_{0.57})O_2$ and our work about the new Li-rich material$Li_{1.13}(Ni_{0.26}Co_{0.09}Mn_{0.52})O_2$, where 3.80 V, 3.70 V, 4.0 V, 3.40 V and 3.55 V discharge median-voltage are assumed for LCO, LNCM523, LMO, LFP, reported Li-rich material respectively based on previous investigation.

Table S1 Equilibrium reactions and constants of the transition metals and chelating agents in the solution.

Equilibrium reaction	log K			
	K	Ni	Mn	Co
$M^{2+}+NH_3 \leftrightarrow [M(NH_3)]^{2+}$	K_1	2.81	1.00	2.10
$M^{2+}+2NH_3 \leftrightarrow [M(NH_3)_2]^{2+}$	K_2	5.08	1.54	3.67
$M^{2+}+3NH_3 \leftrightarrow [M(NH_3)_3]^{2+}$	K_3	6.85	1.70	4.78
$M^{2+}+4NH_3 \leftrightarrow [M(NH_3)_4]^{2+}$	K_4	8.12	1.30	5.53
$M^{2+}+5NH_3 \leftrightarrow [M(NH_3)_5]^{2+}$	K_5	8.93	-	5.75
$M^{2+}+6NH_3 \leftrightarrow [M(NH_3)_6]^{2+}$	K_6	9.08	-	5.14
$M^{2+}+C_2O_4^{2-} \leftrightarrow M(C_2O_4)$	K_1	5.30	3.97	4.79
$M^{2+}+2C_2O_4^{2-} \leftrightarrow [M(C_2O_4)_2]^{2-}$	K_2	7.64	5.80	6.70
$M^{2+}+3C_2O_4^{2-} \leftrightarrow [M(C_2O_4)_3]^{4-}$	K_3	8.50	-	9.70
$M(OH)_2 \leftrightarrow M^{2+}+2OH^-$	K_{sp}	-15.22	-12.7	-14.89
$H_2O \leftrightarrow H^++OH^-$	K_w	-14	-14	-14

Table S2 The simulated results from electrochemical impedance spectra of as-prepared Li-rich oxide electrodes after different cycles.

Sample	Cycle	$R_s(\Omega)$	$R_{ct}(\Omega)$	$W_o(\Omega)$	$W_s(\Omega)$
Normal Li-rich oxide	0	5.178	131.9	24477	54821
	1	2.908	358.1	5326	2843
	10	5.548	42.83	-	2503
New Li-rich oxide	0	3.188	255.6	28920	53383
	1	4.739	446.8	-	9138
	10	3.815	41.62	-	2306

Reference

1 J. R. Ying, C. Y. Jiang and C. R. Wan, *J. Power Sources*, 2004, **129**, 264.

2 P. Y. Hou, X. Q. Wang, J. Guo, J. Zhang, D. W. Song, X. X. Shi, D. G. Wang and L. Q. Zhang, *RSC Adv.*, 2014, **4**, 15923.

3 C. Y. Wan, M. Cheng and D. Wu, *Powder Technology*, 2011, **210**, 47.

4 M. Y. Cho, H. Kim, H. Kim, Y. S. Lim,K. B. Kim, J. W. Lee, K. Kang and K. C.Roh, *J. Mater. Chem. A*, 2014, **2**,5922.

5 H. J.Kima, H. G.Junga, B.Scrosatia and Y. K. Sun, *J. Power Sources*, 2012, **203**, 115.